ORIGINAL RESEARCH

P311 Promotes Lung Fibrosis via Stimulation of Transforming Growth Factor-β1, -β2, and -β3 Translation

Fang-Fang Duan[1], Gabriel Barron[1], Angelo Meliton[2], Gokhan M. Mutlu[2], Nickolai O. Dulin[2], and Lucia Schuger[1]

[1]Department of Pathology and [2]Section of Pulmonary and Critical Care Medicine, Department of Medicine, The University of Chicago Medical School, Chicago, Illinois

Abstract

Interstitial lung fibrosis, a frequently idiopathic and fatal disease, has been linked to the increased expression of profibrotic transforming growth factor (TGF)-βs. P311 is an RNA-binding protein that stimulates TGF-β1, -β2, and -β3 translation in several cell types through its interaction with the eukaryotic translation initiation factor 3b. We report that P311 is switched on in the lungs of patients with idiopathic pulmonary fibrosis (IPF) and in the mouse model of bleomycin (BLM)-induced pulmonary fibrosis. To assess the *in vivo* role of P311 in lung fibrosis, BLM was instilled into the lungs of P311-knockout mice, in which fibrotic changes were significantly decreased in tandem with a reduction in TGF-β1, -β2, and -β3 concentration/activity compared with BLM-treated wild-type mice. Complementing these findings, forced P311 expression increased TGF-β concentration/activity in mouse and human lung fibroblasts, thereby leading to an activated phenotype with increased collagen production, as seen in IPF. Consistent with a specific effect of P311 on TGF-β translation, TGF-β1–, -β2–, and -β3–neutralizing antibodies downregulated P311-induced collagen production by lung fibroblasts. Furthermore, treatment of BLM-exposed P311 knockouts with recombinant TGF-β1, -β2, and -β3 induced pulmonary fibrosis to a degree similar to that found in BLM-treated wild-type mice. These studies demonstrate the essential function of P311 in TGF-β–mediated lung fibrosis. Targeting P311 could prove efficacious in ameliorating the severity of IPF while circumventing the development of autoimmune complications and toxicities associated with the use of global TGF-β inhibitors.

Keywords: lung fibrosis; P311; transforming growth factor-β; fibroblasts; bleomycin

Pulmonary fibrosis is a general term used to describe an increased accumulation of collagen in the distal lung, rendering the lung stiff and compromising its ability to facilitate normal gas exchange. Lung fibrosis can develop as a consequence of occupational or medical exposure, as a result of genetic mutations, connective tissue/rheumatological disease, and after trauma or acute lung injury leading to fibroproliferative acute respiratory distress syndrome, or it can develop in an idiopathic manner. They each result in a progressive loss of lung function with increasing dyspnea, and most forms ultimately result in mortality (1).

Idiopathic pulmonary fibrosis (IPF) is the most prevalent type of fibrotic lung disease, accounting for at least half of all diagnosed cases, and has a natural average survival of 3 years from the time of diagnosis. IPF is more common in males than in females (estimated at 20 in 100,000 for males and 13 in 100,000 for females), and it is viewed as a disease of aging, with the median age at diagnosis being in the mid-60s. IPF manifests with exercise-induced breathlessness, persistent dry cough, and dyspnea, and it is characterized by radiologically evident honeycombing

(Received in original form January 26, 2018; accepted in final form June 24, 2018)

Supported by National Heart, Lung, and Blood Institute grant R01 HL132870 (L.S.).

Author Contributions: F.-F.D.: performed all the studies in the paper two to three times, prepared the figures, and wrote the drafts of the Methods and Results sections and the figure legends; G.B.: performed the studies a third time that F.-F.D. performed twice, as well as repeated the most critical experiments to confirm that these can be replicated by two people; A.M.: taught the bleomycin mouse model to F.-F.D. and G.B. and supervised the first experiments that they performed using the model; G.M.M.: investigator under whom A.M. works; reviewed and discussed the animal experimental design with L.S., and supervised A.M. in the first sets of animal experiments; N.O.D.: taught the bleomycin mouse model to L.S. and provided expert input throughout the project; and L.S.: principal investigator; developed the working hypothesis, designed and supervised all steps of the project, helped F.-F.D. with figure design and improvement of her drafts, and eventually took over and wrote the manuscript.

Correspondence and requests for reprints should be addressed to Lucia Schuger, M.D., Department of Pathology, The University of Chicago Medical School, 5841 South Maryland Avenue, Room J541, Chicago, IL 60637. E-mail: lschuger@bsd.uchicago.edu.

This article has a data supplement, which is accessible from this issue's table of contents at www.atsjournals.org.

Am J Respir Cell Mol Biol Vol 60, Iss 2, pp 221–231, Feb 2019

Originally Published in Press as DOI: 10.1165/rcmb.2018-0028OC on September 21, 2018
Internet address: www.atsjournals.org

and the histological pattern of usual interstitial pneumonia (2–4). The key features of usual interstitial pneumonia include fibrotic lung remodeling with temporal heterogeneity, hyperplastic type II alveolar epithelial cells lining areas of fibrosis, presence of fibroblastic foci (activated fibroblasts), minor amounts of inflammation, and thickening of the interalveolar septa.

Subsequent to the failure of multiple therapeutic approaches, two drugs were found to slow the progression of the disease, namely nintedanib, an inhibitor of multiple tyrosine kinases, and pirfenidone, which works by reducing the production of procollagens I and II (2–4). However, the prognosis for patients with IPF remains poor, and the search continues for drugs that inhibit the pathogenic pathways active in IPF to reduce or even halt the progression of the disease (2–4).

Despite the remarkable heterogeneity in the etiological mechanisms responsible for the development of fibrotic diseases and their clinical manifestations, numerous studies have identified critical signaling cascades initiated primarily by transforming growth factor (TGF)-β1 as a common element responsible for the development of profibrotic reactions (5), including IPF (6, 7). Like TGF-β1 (8–10), TGF-β2 and TGF-β3 are also increased in IPF (11, 12). TGF-β2 has been shown to promote fibrosis (13–17), but there is controversy regarding TGF-β3. Researchers in several studies reported that TGF-β3 has a protective effect against fibrosis (18–20), a view that gained some support (21, 22). However, in contrast, a larger number of reports attributed a profibrogenic effect to TGF-β3 (17, 23–26). In support of this latter view, recombinant (r)TGF-β3 (avotermin) had no antiscarring effect in clinical trials (27).

P311 is an 8 kD, conserved, RNA-binding protein with restricted cell expression. As such, P311 is steadily expressed in vascular and visceral smooth muscle beds (28) and in the nervous system (28, 29). It is transiently expressed in regenerating tissues (30–33) and several pathological settings, such as hypertrophic scars (17, 34), renal fibrosis (35), and malignant glioblastomas (36). Among its biological functions, P311 induces myofibroblast differentiation and migration (30, 37), promotes nerve and lung regeneration (31, 32), and is essential for the maintenance of normal blood pressure (28) and the development of normal cutaneous scars (17). In addition, behavioral studies suggested that P311-knockout (P311-KO) mice may have impaired memory and emotional/affective responses (38, 39).

At the molecular level, P311 is required for the optimal translation of TGF-β1, -β2, and -β3 (28, 40). Because P311 is an intrinsically disordered protein (40), it requires an interacting partner(s) to acquire tertiary structure and function. Eukaryotic translation initiation factor 3 subunit b (eIF3b) is the best characterized P311-binding partner identified so far (40). The eIF3b–P311 binding sites were mapped to the noncanonical RNA recognition motif of eIF3b and a central 11–amino acid region of P311 referred to as an *eIF3b-binding motif*. Through its concomitant binding to eIF3b and to the 5′ untranslated region of TGF-β1, -β2, and -β3 mRNAs, P311 recruits TGF-β1, -β2, and -β3 mRNAs to the translation machinery, which in turn leads to their increased translation (40). P311 is therefore the first documented regulator of all three TGF-βs and the only protein currently known to stimulate TGF-β translation *in vitro* and *in vivo* (28, 40).

With this information in hand, we elected to examine the potential role of P311 in pulmonary fibrosis. In this article, we report that P311 is present in IPF as well as in bleomycin (BLM)-induced lung fibrosis, whereas it is not detectable in normal lung parenchyma, except for bronchial and vascular smooth muscle cells. We used the acute BLM mouse model of pulmonary fibrosis, P311-KO and wild-type (WT) mice, and primary cultures of mouse and human lung fibroblasts (MLFs and HLFs, respectively) to examine the potential involvement of P311 in the lung fibrogenic process. Altogether, these studies demonstrate that by promoting TGF-β1, -β2, and -β3 translation, P311 plays an essential role in the pathogenesis of lung scarring and point to the lung fibroblasts as important P311 effector cells. Of potential therapeutic relevance, we observed that P311 ablation reduces but does not eliminate TGF-β1, -β2, and -β3 production. Therefore, targeting P311 could have the advantage of eliminating the autoimmune complications and multiple toxicities associated with the complete abolishment of TGF-β signaling (41).

Methods

P311 Detection in IPF

P311 expression in lung tissues from six cases of IPF and from six matching control subjects was examined by immunohistochemistry (IHC). The immunostaining was performed at the University of Chicago Pathology Tissue Core Facility using a Leica BOND-MAX automated IHC/*in situ* hybridization system (Leica Microsystems) and the BOND Polymer Refine detection system (Leica Microsystems) as previously described (42). Briefly, formalin-fixed, paraffin-embedded, 5-μm tissue sections were boiled for 20 minutes in fresh citrate buffer for antigen retrieval and incubated for 25 minutes with an antihuman P311 antibody (17) at 1:50 dilution, followed by a PBS wash for 15 minutes, BOND polymer horseradish peroxidase incubation for 25 minutes, and then incubation with peroxidase blocking solution for 5 minutes. The peroxidase reaction was developed using 3,3′-diaminobenzidine provided with the kit (Abcam), followed by counterstaining with hematoxylin for 5 minutes.
Last, the slides were dehydrated in increasing concentrations of alcohol and mounted in mounting medium (Life Technologies).

Mice

The generation of P311-KO mice (C57BL/6 mice with deletion of the entire P311 coding region on both alleles) was previously described (38). Male P311-KO and WT C57BL/6 mice weighing 22–25 g (7–9 wk old; The Jackson Laboratory) were used in this study. The animals were housed at the University of Chicago Animal Facility at 25°C room temperature on a 12-hour light cycle and supplied with rodent diet no. 2918 (18% protein, 6% fat, and moderate phytoestrogen; Harlan Laboratories). All studies involving animals were reviewed and approved by our institution's institutional animal care and use committee.

BLM-induced Model of Pulmonary Fibrosis

Mice were anesthetized with an intraperitoneal injection of ketamine/xylazine (ketamine, 80 mg/kg; xylazine, 10 mg/kg). BLM sulfate (Gold

Biotechnology) was then administered by intratracheal instillation as a single dose of 2 U/kg in 50 μl of sterile PBS solution. Control mice received an equal volume of sterile PBS solution. To facilitate equal distribution of BLM within the whole lung, each mouse was gently rotated left and right several times (based on preliminary studies instilling India ink). Body weights and mortality were monitored throughout the whole experiment. Two weeks after instillation of BLM, the animals were killed, and their lungs were removed for further studies.

BAL Fluid Analysis

BAL fluid (BALF) analysis was performed before mice were killed as previously described (43). Briefly, the animals were anesthetized with an intraperitoneal injection of ketamine/xylazine (ketamine, 80 mg/kg; xylazine, 10 mg/kg). The trachea was then exposed and intubated with a plastic catheter (18-gauge; Kimble Chase). Two repeated injections of PBS (0.5 ml) were subsequently instilled through the catheter to collect the BALF. The BALF was then centrifuged at 300 *g* for 10 minutes at 4°C, and the supernatant was frozen at −80°C for subsequent studies.

Cell Culture

Primary MLFs (American Type Culture Collection) and primary HLFs (Lonza) were seeded onto culture tissue plastic dishes and were cultured in Eagle's minimum essential medium (American Type Culture Collection) and fibroblast basal medium (Lonza), respectively, both containing 10% FBS (HyClone Laboratories), 2 mmol/L L-glutamine (Thermo Fisher Scientific), and antibiotic-antimycotic reagent (Anti-Anti; Thermo Fisher Scientific), and were incubated at 37°C in an atmosphere of 95% air and 5% CO_2. *See* the Supplemental Materials and Methods section of the data supplement for further details.

Results

P311 Is Expressed in IPF and in the Mouse Model of BLM-induced Pulmonary Fibrosis

IHC studies did not detect P311 (brown color) in normal human lungs (Figures 1A and 1B), except for the muscle layer of airways and blood vessels (Figure 1B, arrows). However, in IPF, P311 was detected in hyperplastic type II alveolar epithelial cells (Figure 1C, arrow) and activated fibroblasts (fibroblastic focus) (Figure 1D) in addition to its normal detection in lung smooth muscle cells.

The BLM-treated mice lost 5–10% of their body weight and exhibited no mortality. Western blot analysis revealed that P311 was abundant in the lungs of BLM-treated WT mice, whereas it was weakly detected in the lungs of matched PBS-treated counterparts owing to the normal presence of P311 in vascular and bronchial smooth muscle cells (Figure 1E).

Lack of P311 Results in Decreased Collagen Deposition in the Mouse Model of BLM-induced Pulmonary Fibrosis

Masson's trichrome staining demonstrated a decrease in the amount of interstitial collagen fibril deposition (blue color) in the lungs of BLM-treated P311-KO mice compared with that of BLM-treated WT mice (Figure 2A). This observation was confirmed by quantification of blue-stained collagen fibrils using the Aperio ScanScope CS System (Figure 2A, graph to the right of microphotographs). Consistently, hydroxyproline (HYP) incorporation assays showed decreased collagen production in the lungs of BLM-treated P311-KO mice (Figure 2B). qPCR analysis showed a

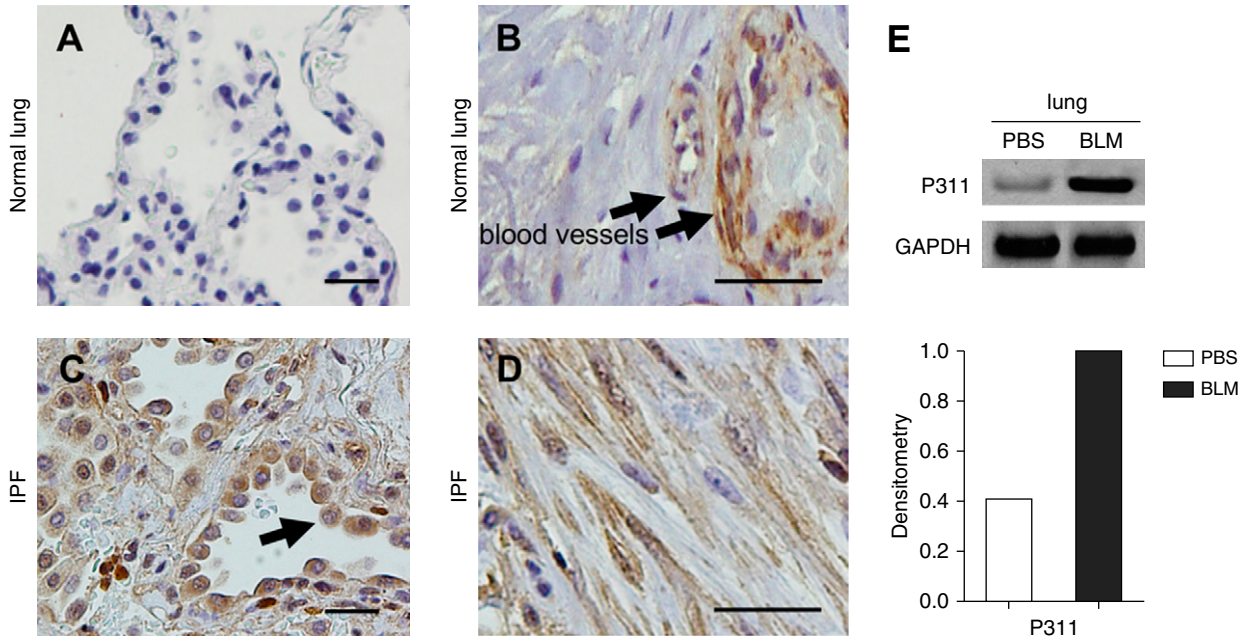

Figure 1. P311 expression is switched on in IPF and in a mouse model of BLM-induced pulmonary fibrosis. (*A–D*) Immunohistochemical detection of P311 (brown color) in normal human lung (*A* and *B*) and in IPF (*C* and *D*). Scale bars: 100 μm. Arrows point to blood vessel muscular layer (normally positive for P311) in *B* and to hyperplastic type II alveolar epithelial cells in *C*. (*D*) Activated fibroblasts (fibroblastic focus). (*E*) Western blot analysis with corresponding densitometry showing P311 in PBS-treated and BLM-treated mouse lungs at 2 weeks after treatment. $n = 6$ mice per group. BLM = bleomycin; IPF = idiopathic pulmonary fibrosis.

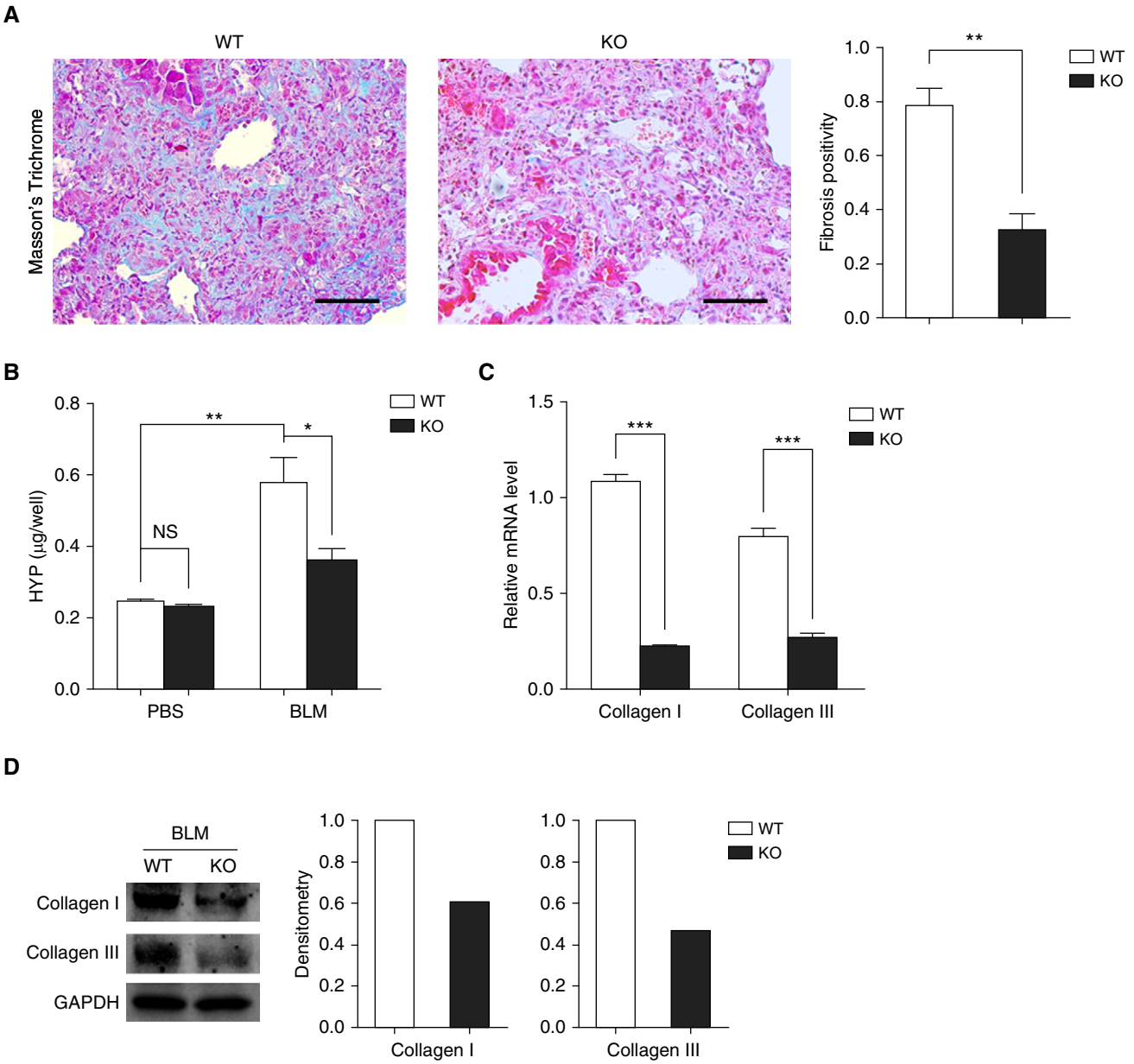

Figure 2. Lack of P311 results in decreased collagen deposition in a mouse model of BLM-induced pulmonary fibrosis. (*A*) Masson trichrome collagen detection (blue color) in lungs from BLM-treated WT and P311-KO mice. Scale bars: 100 μm. Quantification of blue-stained collagen fibrils is shown in the graph to the right of microphotographs. Quantitative total percentage of positivity (total number of positive pixels divided by total number of pixels). (*B*) HYP incorporation in lungs from BLM-treated WT and P311-KO mice. (*C*) qPCR showing mRNA concentrations of collagen I and collagen III in lungs from BLM-treated WT and P311-KO mice. (*D*) Western blot analysis and corresponding densitometry showing collagen I and collagen III in lungs from BLM-treated WT and P311-KO mice. All these studies were performed 2 weeks after BLM treatment. Data are represented as mean ± SD. $n = 6$ mice per group, $^{*}P < 0.005$; $^{**}P < 0.01$; $^{***}P < 0.001$. HYP = hydroxyproline; KO = knockout; NS = not significant; WT = wild type.

decrease in collagen I and collagen III mRNA concentrations in BLM-treated P311-KO mice (Figure 2C). Similarly, Western blots demonstrated a decrease in collagen I and collagen III protein concentrations in P311-KO mice compared with WT mice after BLM treatment (Figure 2D).

Lack of P311 Results in Decreased Lung TGF-β1, -β2, and -β3 Concentration/Activity in the Mouse Model of BLM-induced Pulmonary Fibrosis

qPCR showed no significant differences in lung TGF-β1, -β2, and -β3 mRNA concentrations between BLM-treated WT and P311-KO mice (Figure 3A). However, Western blot analysis revealed a decrease in pulmonary concentrations of pro–TGF-β1, -β2, and -β3 in BLM-treated P311-KO mice compared with WT mice (Figure 3B). ELISA also demonstrated a significant decrease in the concentrations of total TGF-β1, -β2, and -β3 in the lungs of BLM-treated P311-KO

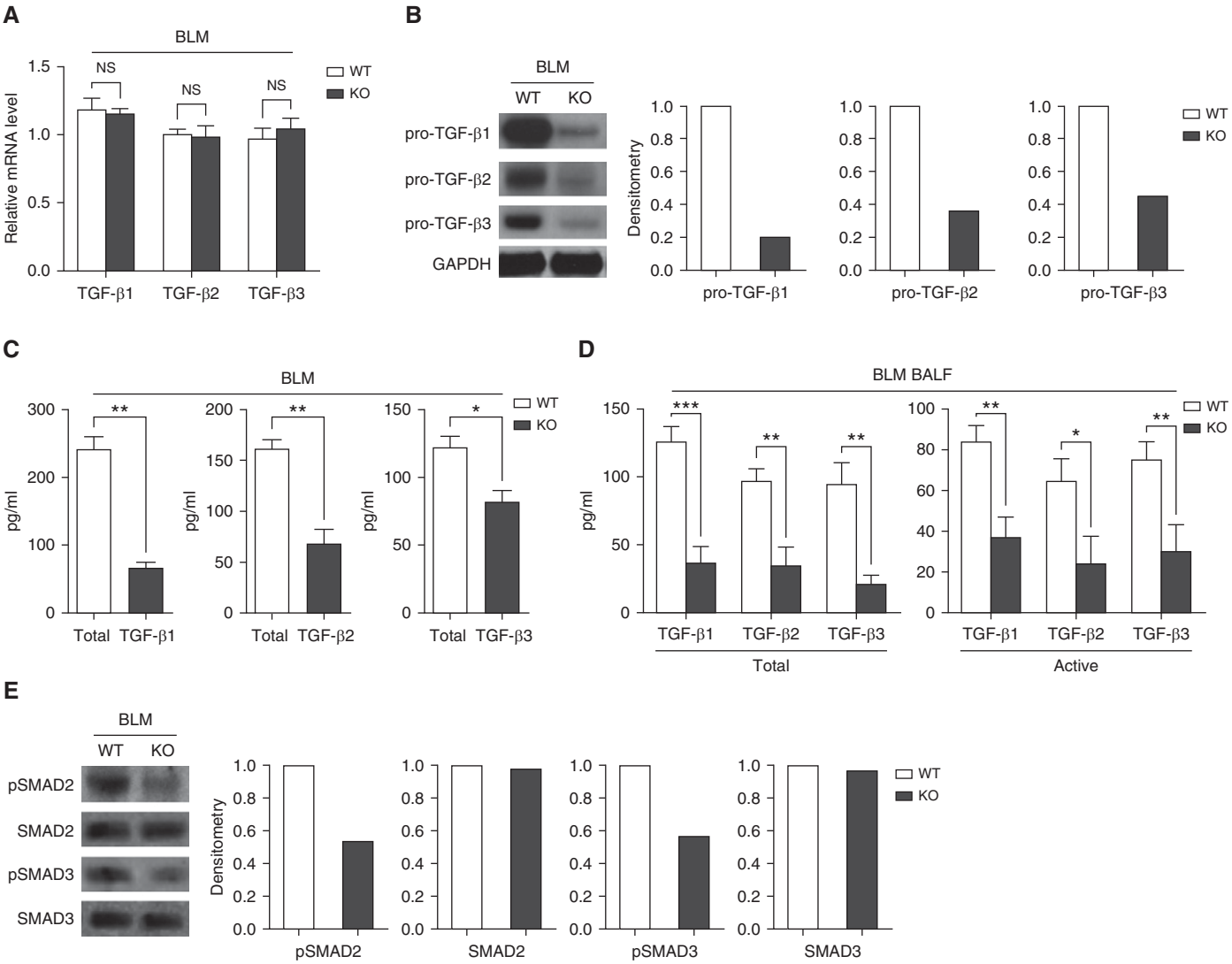

Figure 3. Lack of P311 results in decreased TGF-β1, -β2, and -β3 concentration/activity with no change in corresponding mRNA concentrations in a mouse model of BLM-induced pulmonary fibrosis. (*A*) qPCR showing mRNA concentrations of TGF-β1, -β2, and -β3 in the lungs from WT and P311-KO mice. (*B*) Western blot analysis and corresponding densitometry showing pro–TGF-β1, -β2, and -β3 in the lungs from WT and P311-KO mice. (*C*) ELISAs showing total TGF-β1, -β2, and -β3 in the lungs from WT and P311-KO mice. (*D*) ELISAs showing total and active TGF-β1, -β2, and -β3 in the BALF from WT and P311-KO mice. (*E*) Western blot analysis and corresponding densitometry showing SMAD2 and SMAD3 (total) concentrations and pSMAD2 and pSMAD3 (active) levels in the lungs from WT and P311-KO mice. All these studies were performed 2 weeks after BLM treatment. Data are represented as mean ± SD. $n = 3$ mice per group in *A*; $n = 4$ mice per group in *B* and *C*; $n = 6$ mice per group in *D* and *E*. $^{*}P < 0.05$; $^{**}P < 0.01$; $^{***}P < 0.001$. BALF = BAL fluid; p = phosphorylated; TGF = transforming growth factor.

mice (Figure 3C). Because the concentrations of active TGF-β cannot be determined in tissue lysates, we performed ELISAs to measure total and active TGF-β1, -β2, and -β3 concentrations in BALF collected from BLM-treated P311-KO and WT mice. These studies revealed decreased total and active TGF-β1, -β2, and -β3 concentrations in the BALF of BLM-treated P311-KO mice (Figure 3D). We further determined the SMAD2 and SMAD3 phosphorylation levels in the lungs of BLM-treated P311-KO and WT mice as an indication of TGF-β activation. Western blot analysis showed reduced phosphorylated (p)SMAD2 and pSMAD3 concentrations without changes in total SMAD2 and SMAD3 concentrations in BLM-treated P311-KO mice compared with WT mice (Figure 3E).

P311 Stimulates Collagen Production by Lung Fibroblasts

qPCR showed increased collagen I and collagen III mRNA concentrations in Myc-tagged P311-transfected MLFs and HLFs compared with empty vector (EV)-transfected controls (Figure 4A). Consistent with these findings, immunoblot analysis revealed increased collagen I and collagen III concentrations in Myc-tagged P311-transfected MLFs and HLFs (Figures 4B and 4C).

P311 Profibrotic Effect Results from Upregulation of TGF-β1, -β2, and -β3 Concentration/Activity in Lung Fibroblasts

As observed *in vivo*, qPCR showed no significant differences in TGF-β1, -β2,

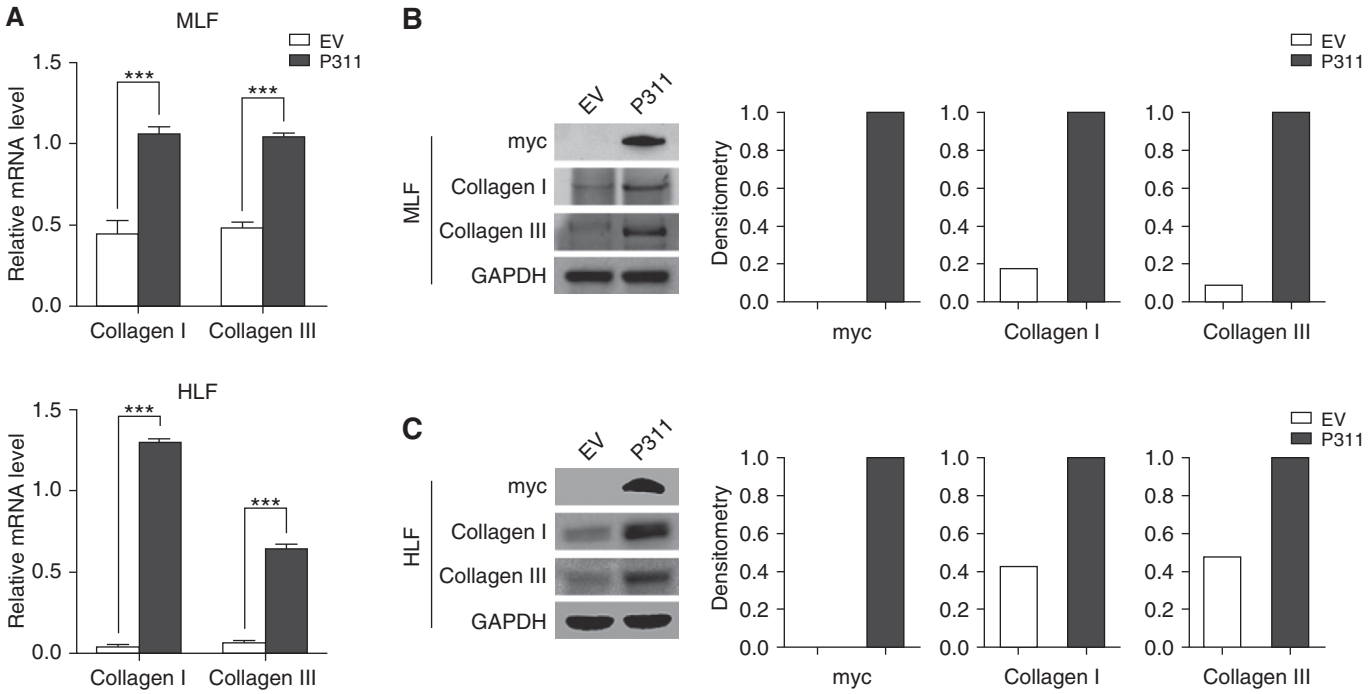

Figure 4. P311 stimulates collagen production by lung fibroblasts. (*A*) qPCR showing concentrations of collagen I and collagen III mRNAs in MLFs and HLFs transfected with EV or Myc-tagged P311. (*B*) Western blot analysis and corresponding densitometry showing collagen I and collagen III expression in MLFs transfected with EV or Myc-tagged P311. (*C*) Western blot analysis and corresponding densitometry showing collagen I and collagen III expression in HLFs transfected with EV or Myc-tagged P311. Data are represented as mean ± SD. $n = 4$ replicates per group in *A*; $n = 3$ replicates per group in *B* and *C*. ***$P < 0.001$. EV = empty vector; HLF = human lung fibroblast; MLF = mouse lung fibroblast.

and -β3 mRNA concentrations between MLFs and HLFs transfected with EV or Myc-tagged P311 (Figure 5A). However, ELISAs showed increased concentrations of total TGF-β1, -β2, and -β3 in Myc-tagged P311-transfected MLFs and HLFs when compared with EV-transfected controls (Figures 5B and 5C). Moreover, the P311-mediated increase in TGF-β1, -β2, and -β3 concentrations resulted in an increase in their activity, as indicated by increased pSMAD2 and pSMAD3 concentrations without changes in total SMAD2 and SMAD3 in Myc-tagged P311-transfected MLFs and HLFs compared with their control counterparts (*see* Figures E1A and E1B in the data supplement).

To conclusively determine that the profibrotic effect of P311 was dependent on TGF-β1, -β2, and -β3 upregulation, neutralizing TGF-β1, 2, and 3 antibodies were added to MLFs and HLFs after transfection with EV or Myc-tagged P311. Immunoblot analysis showed that, indeed, TGF-βs blockage reversed the P311-mediated increase in collagen I and collagen III concentrations (Figures 5D and 5E).

P311 Promotes an Activated Lung Fibroblast Phenotype

Bromodeoxyuridine incorporation assays demonstrated an increase in the proliferation of Myc-tagged P311-transfected MLFs and HLFs compared with EV-transfected controls (Figures 6A and 6B). Collagen gel contraction assays showed increased cell contractility in Myc-tagged P311-transfected MLFs and HLFs (Figures 6C and 6D). Finally, cell migration assays showed an increase in the migration of Myc-tagged P311-transfected MLFs and HLFs compared with their EV-transfected controls (Figures 6E and 6F).

Exogenous TGF-β1, -β2, and -β3 Ameliorate the Collagen Deficit in Lungs of BLM-treated P311-KO Mice

HYP incorporation assays performed on lung tissue after intraperitoneal injection of rTGF-βs, administered to P311-KO mice, and of PBS, administered to WT mice, demonstrated similar amounts of collagen in the lungs of WT and rTGF-β1–treated P311-KO mice (Figure 7A) and a statistically significant increase in collagen production in the lungs of rTGF-β2– and rTGF-β3–treated P311-KO mice (Figures 7B and 7C).

Discussion

Pulmonary fibrosis involves the gradual accumulation of collagen in the distal lung, compromising its ability to facilitate normal gas exchange. IPF is the most prevalent type of fibrotic lung disease, accounting for at least half of all diagnosed cases. Two new drugs, nintedanib and pirfenidone, are currently used to reduce the progression of the disease (44–46). However, the prognosis for patients with IPF remains poor, and efforts to elucidate its pathogenesis continue with the hope of coming up with better treatment options (3).

TGF-β, the most powerful fibrogenic growth factor discovered to date (5), plays a critical role in the development and progression of all forms of fibrosis, regardless of their etiology (4–7, 47–53). Because we previously found that P311 stimulates the translation of all three TGF-βs in smooth muscle (28), NIH-3T3 cells, and skin fibroblasts (17, 40), in the present study, we sought to determine whether

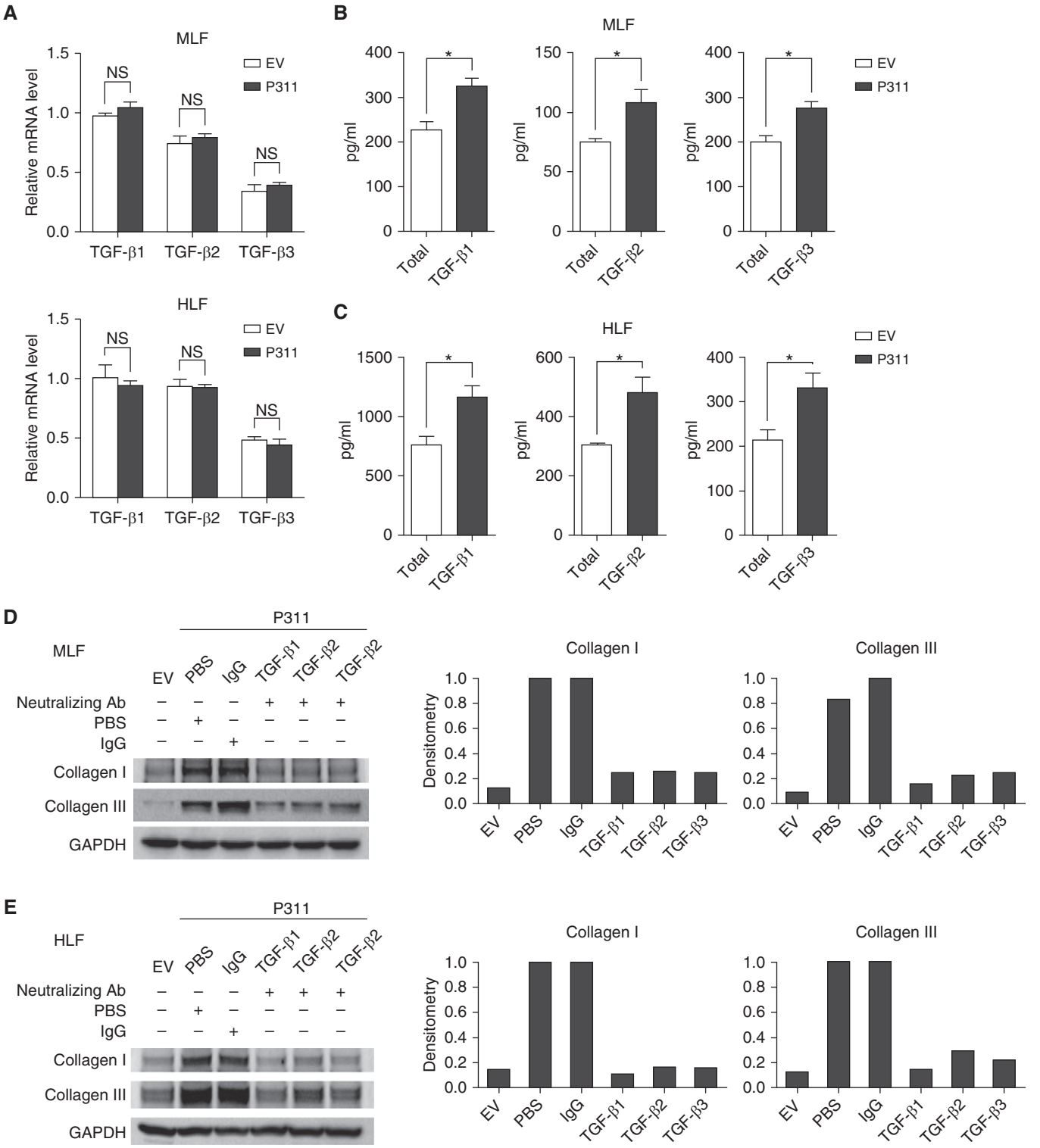

Figure 5. P311 profibrotic effects are mediated by upregulation of TGF-β1, -β2, and -β3 concentrations. (*A*) qPCR showing mRNA concentrations of TGF-β1, -β2, and -β3 in MLFs and HLFs transfected with EV or Myc-tagged P311. (*B* and *C*) ELISAs showing concentrations of total TGF-β1, -β2, and -β3 in MLFs and HLFs transfected with EV or Myc-tagged P311. (*D*) Western blot analysis and corresponding densitometry showing collagen I and collagen III concentrations after TGF-β1, -β2, and -β3 blockage using neutralizing antibodies in MLFs transfected with EV or Myc-tagged P311. Readers may view the uncut gels for *D* in the data supplement. (*E*) Western blot analysis and corresponding densitometry showing collagen I and collagen III concentrations after TGF-β1, -β2, and -β3 blockage using neutralizing antibodies in HLFs transfected with EV or Myc-tagged P311. Data are presented as mean ± SD. $n = 4$ replicates per group in *A–C*; $n = 3$ replicates per group in *D* and *E*. *$P < 0.05$. Ab = antibody.

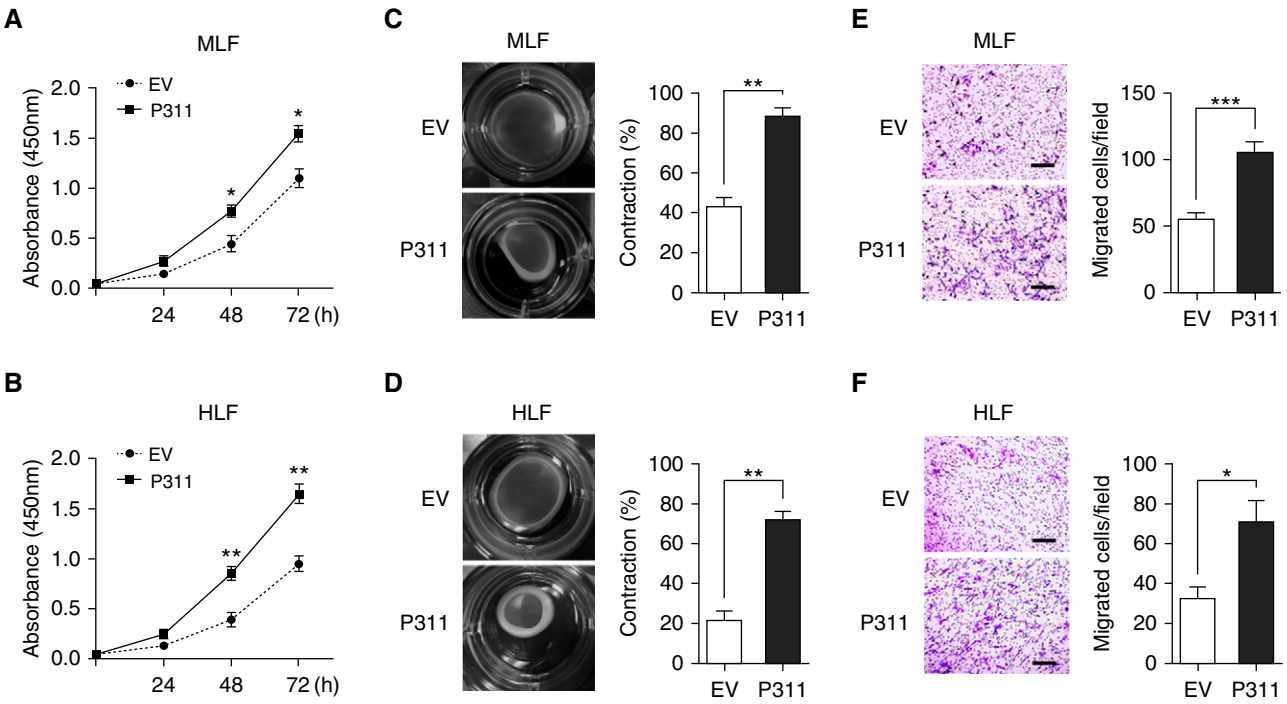

Figure 6. P311 activates lung fibroblasts. (*A* and *B*) Bromodeoxyuridine incorporation assays of MLFs and HLFs transfected with EV or Myc-tagged P311. (*C* and *D*) Collagen gel contraction by MLFs and HLFs transfected with EV or Myc-tagged P311. (*E* and *F*) Transwell migration assay of MLFs and HLFs transfected with EV or Myc-tagged P311. Scale bars: 100 μm. Data are represented as mean ± SD. $n = 4$ replicates per group in *A* and *B;* $n = 3$ replicates per group in *C* and *D*; $n = 4$ replicates per group in *E* and *F*. $^{*}P < 0.05$; $^{**}P < 0.01$; $^{***}P < 0.001$.

P311 might be involved in TGF-β–mediated lung fibrosis.

Because no publications to date had examined the role of P311 in the pulmonary system, in our first set of studies, we assessed its expression in normal and fibrotic human and mouse lungs. The latter was represented by the animal model of acute BLM-induced pulmonary fibrosis, which, although far from an accurate recapitulation of IPF mechanisms and characteristics, remains the best available experimental tool for studying disease pathogenesis (54) and for testing novel pharmaceutical compounds (55, 56).

IHC and Western blotting showed that P311 is not detectable in normal human and murine lungs (except for the muscle layers of blood vessels and airways); however, it becomes highly expressed in reactive fibroblasts and alveolar epithelial cells in IPF and in the lungs of mice exposed to intratracheally delivered BLM, a finding consistent with a potential role for P311 in the pathogenesis of pulmonary fibrosis.

To explore such a possibility, we further examined the lungs of BLM-treated

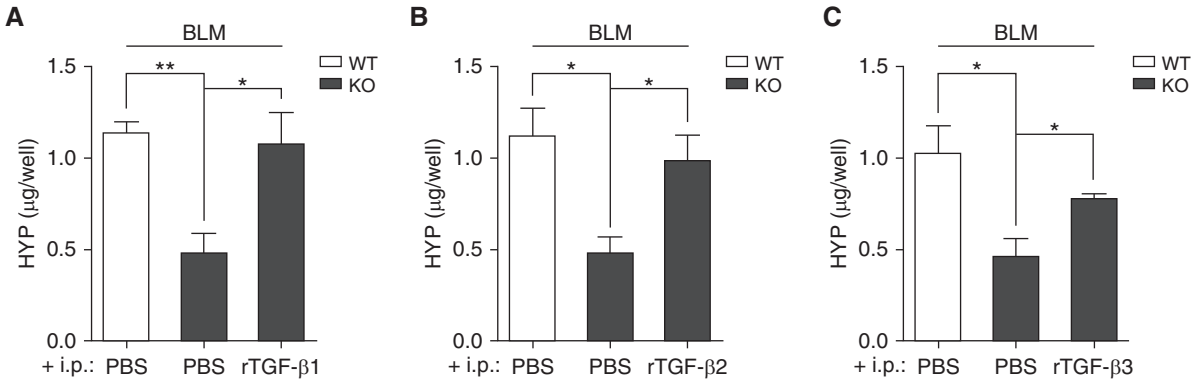

Figure 7. Supplementation with TGF-β1, -β2, or -β3 rescues the deficit in collagen in the lungs of BLM-treated P311-KO mice. (*A*) HYP incorporation by lungs from BLM-treated WT mice given i.p. injections with PBS and by lungs from BLM-treated P311-KO mice given i.p. injections with PBS and rTGF-β1. (*B*) HYP incorporation by lungs from BLM-treated WT mice given i.p. injections with PBS and by lungs from BLM-treated P311-KO mice given i.p. injections with PBS and rTGF-β2. (*C*) HYP incorporation by lungs from BLM-treated WT mice given i.p. injections with PBS and by lungs from BLM-treated P311-KO mice given i.p. injections with PBS and rTGF-β3. Data are represented as mean ± SD. $n = 6$ mice per group. $^{*}P < 0.05$; $^{**}P < 0.01$. r = recombinant.

P311-KO and WT mice using established fibrogenesis parameters, including Masson's trichrome staining and quantification, HYP incorporation assays, and qPCR plus immunoblot analysis for collagen I and collagen III. All these studies consistently demonstrated a significant decrease in collagen production and deposition in the lungs of P311-KO mice. Although previous reports by researchers at our laboratory and others attributed a profibrogenic role to P311 in cutaneous and renal scarring, respectively (17, 57), this was the first indication that P311 plays a similar function in the lung.

To determine whether the effect of P311 in the context of lung fibrosis is accomplished by the stimulation of TGF-β translation, we assessed TGF-β mRNA and protein concentrations in the lungs of BLM-treated P311-KO and WT mice. qPCR showed no significant differences in TGF-β1, -β2, and -β3 mRNA concentrations between these two sets of animals; however, immunoblotting and ELISAs revealed a decrease in the total concentrations of TGF-β1, -β2, and -β3 in P311-KO mice. Because P311 is not involved in the degradation of TGF-β (28, 40), the lack of changes in TGF-β mRNA, together with the decrease in the corresponding protein products, indicated that pulmonary P311 acts at the TGF-β translation level, as we previously found in other biological contexts in which the P311 effect was confirmed by TGF-β translation reporter assays (17, 40).

Our findings differed from those reported by another group that indicated a P311-mediated increase in *Tgfβ1* transcription in myofibroblasts (35) and in epidermal stem cells (58). Although this discrepancy could be due to the difference in cell type, we note that these investigators paradoxically reported a concomitant decrease in TGF-β1 mRNA concentrations in tandem with the P311-mediated increase in transcription. Furthermore, this group reported the effect in *Tgfβ1* transcription to be mediated by the binding of P311 with eukaryotic initiation factor 6, a ribosomal protein critical for mRNA translation (35). Interestingly, in another publication by the same group, this time focused on renal fibrosis, a discrepancy between TGF-β1 mRNA and protein concentrations coincident with our observations was reported (57).

Because total and active TGF-βs oftentimes are not correlated (59, 60), and because active TGF-βs cannot be detected in cells or tissues, we next determined the concentrations of active TGF-β1, -β2, and -β3 in BALF collected from BLM-treated P311-KO and WT mice using ELISAs. These studies revealed a reduction in both total and active TGF-β1, -β2, and -β3 concentrations in P311-KO mice. Confirming the decrease in TGF-β1, -β2, and -β3 activity, Western blot analysis showed reduced pSMAD2 and pSMAD3 without changes in total SMAD2 and SMAD3 in BLM-treated P311-KO mice.

To begin to probe the function of P311 at the cellular level, we conducted studies using primary cultures of MLFs and HLFs. We previously reported that P311 stimulates TGF-β translation in skin fibroblasts (17). However, because important fibroblast biological characteristics differ in a tissue- and organ-specific manner (61–63), we first confirmed that P311 transfectants are capable of stimulating TGF-β1, -β2, and -β3 translation in MLFs and HLFs, cells in which P311 is not detected under normal conditions. We then found that collagen I and collagen III mRNA and protein concentrations increased in Myc-tagged P311-transfected MLFs and HLFs compared with EV-transfected controls, and the collagen increment was eliminated by TGF-β1, -β2, and -β3 blocking antibodies. Hence, these *in vitro* studies suggested that the P311 profibrogenic function observed *in vivo* was at least in part mediated by P311-induced upregulation of TGF-β concentration/activity in lung fibroblasts. The importance of fibroblasts as effectors of TGF-β–induced pulmonary fibrosis was recently highlighted by a study showing that fibroblast-specific inhibition of TGF-β signaling through the use of trihydroxyphenolic compounds significantly attenuated lung fibrosis in animal models (53).

To continue our *in vitro* characterization effort, we performed functional studies. These showed that P311 stimulated proliferation, promoted migration, and increased contractility of both MLFs and HLFs, all consistent with the induction of an activated state (64), as seen in IPF (65, 66). Overall, the observed P311-induced fibroblast responses paved the way for better understanding of how P311 facilitates lung fibrosis.

Finally, HYP incorporation assays performed on lung tissues from BLM-treated WT and P311-KO mice after rTGF-β1, rTGF-β2, and rTGF-β3 supplementation demonstrated that each of the TGF-βs either eliminated or reduced in a statistically significant manner the collagen deficit observed in the absence of P311, confirming our *in vitro* observation that TGF-βs are the downstream effectors of P311-mediated lung fibrosis. In addition, our findings stand against the widespread view that TGF-β3 acts as an antifibrogenic factor (21, 22).

On the basis of our present data, we conclude that P311 expression is switched on in the context of IPF and BLM-induced lung fibrosis, in which it plays a critical profibrogenic role by stimulating TGF-β1, -β2, and -β3 translation in pulmonary fibroblasts. Unlike all pan–TGF-β suppression approaches that have undergone or are currently undergoing clinical trials (41), targeting P311 could have the unique advantage of reducing but not eliminating TGF-β concentrations, thereby preventing the development of autoimmune complications and multiple toxicities associated with the complete abolishment of TGF-β signaling (41). ■

Author disclosures are available with the text of this article at www.atsjournals.org.

References

1. Wells AU, Denton CP. Interstitial lung disease in connective tissue disease—mechanisms and management. *Nat Rev Rheumatol* 2014; 10:728–739.
2. Nathan SD. Evaluating new treatment options. *Am J Manag Care* 2017; 23(11, Suppl):S183–S190.
3. Kolb M, Bonella F, Wollin L. Therapeutic targets in idiopathic pulmonary fibrosis. *Respir Med* 2017;131:49–57.
4. Walton KL, Johnson KE, Harrison CA. Targeting TGF-β mediated SMAD signaling for the prevention of fibrosis. *Front Pharmacol* 2017;8:461.
5. Rosenbloom J, Macarak E, Piera-Velazquez S, Jimenez SA. Human fibrotic diseases: current challenges in fibrosis research. *Methods Mol Biol* 2017;1627:1–23.

6. Oruqaj G, Karnati S, Vijayan V, Kotarkonda LK, Boateng E, Zhang W, *et al*. Compromised peroxisomes in idiopathic pulmonary fibrosis, a vicious cycle inducing a higher fibrotic response via TGF-β signaling. *Proc Natl Acad Sci USA* 2015;112:E2048–E2057.
7. Boehme SA, Franz-Bacon K, DiTirro DN, Ly TW, Bacon KB. MAP3K19 is a novel regulator of TGF-β signaling that impacts bleomycin-induced lung injury and pulmonary fibrosis. *PLoS One* 2016;11:e0154874.
8. Haug C. Exit [in Norwegian]. *Tidsskr Nor Laegeforen* 2009;129:1843.
9. Bergeron A, Soler P, Kambouchner M, Loiseau P, Milleron B, Valeyre D, *et al*. Cytokine profiles in idiopathic pulmonary fibrosis suggest an important role for TGF-β and IL-10. *Eur Respir J* 2003;22:69–76.
10. Tomasek JJ, Gabbiani G, Hinz B, Chaponnier C, Brown RA. Myofibroblasts and mechano-regulation of connective tissue remodelling. *Nat Rev Mol Cell Biol* 2002;3:349–363.
11. Hinata N, Takemura T, Ikushima S, Yanagawa T, Ando T, Okada J, *et al*. Phenotype of regenerative epithelium in idiopathic interstitial pneumonias. *J Med Dent Sci* 2003;50:213–224.
12. Hirabayashi T, Demertzis S, Schäfers J, Hoshino K, Nashan B. Chronic rejection in lung allografts: immunohistological analysis of fibrogenesis. *Transpl Int* 1996;9(Suppl 1):S293–S295.
13. Biressi S, Miyabara EH, Gopinath SD, Carlig PM, Rando TA. A Wnt-TGFβ2 axis induces a fibrogenic program in muscle stem cells from dystrophic mice. *Sci Transl Med* 2014;6:267ra176.
14. Echeverría C, Montorfano I, Tapia P, Riedel C, Cabello-Verrugio C, Simon F. Endotoxin-induced endothelial fibrosis is dependent on expression of transforming growth factors β1 and β2. *Infect Immun* 2014;82:3678–3686.
15. Ma B, Kang Q, Qin L, Cui L, Pei C. TGF-β2 induces transdifferentiation and fibrosis in human lens epithelial cells via regulating gremlin and CTGF. *Biochem Biophys Res Commun* 2014;447:689–695.
16. Wang B, Koh P, Winbanks C, Coughlan MT, McClelland A, Watson A, *et al*. miR-200a prevents renal fibrogenesis through repression of TGF-β2 expression. *Diabetes* 2011;60:280–287.
17. Cheng T, Yue M, Aslam MN, Wang X, Shekhawat G, Varani J, *et al*. Neuronal protein 3.1 deficiency leads to reduced cutaneous scar collagen deposition and tensile strength due to impaired transforming growth factor-β1 to -β3 translation. *Am J Pathol* 2017; 187:292–303.
18. Shah M, Foreman DM, Ferguson MW. Neutralisation of TGF-β1 and TGF-β2 or exogenous addition of TGF-β3 to cutaneous rat wounds reduces scarring. *J Cell Sci* 1995;108:985–1002.
19. Xu L, Xiong S, Guo R, Yang Z, Wang Q, Xiao F, *et al*. Transforming growth factor β3 attenuates the development of radiation-induced pulmonary fibrosis in mice by decreasing fibrocyte recruitment and regulating IFN-γ/IL-4 balance. *Immunol Lett* 2014;162:27–33.
20. Guo X, Hutcheon AE, Zieske JD. Molecular insights on the effect of TGF-β1/-β3 in human corneal fibroblasts. *Exp Eye Res* 2016;146: 233–241.
21. Profyris C, Tziotzios C, Do Vale I. Cutaneous scarring: pathophysiology, molecular mechanisms, and scar reduction therapeutics. Part I. The molecular basis of scar formation. *J Am Acad Dermatol* 2012;66:1–10, quiz 11–12.
22. Lichtman MK, Otero-Vinas M, Falanga V. Transforming growth factor β (TGF-β) isoforms in wound healing and fibrosis. *Wound Repair Regen* 2016;24:215–222.
23. Papakonstantinou E, Aletras AJ, Roth M, Tamm M, Karakiulakis G. Hypoxia modulates the effects of transforming growth factor-β isoforms on matrix-formation by primary human lung fibroblasts. *Cytokine* 2003;24:25–35.
24. Lu L, Saulis AS, Liu WR, Roy NK, Chao JD, Ledbetter S, *et al*. The temporal effects of anti-TGF-β1, 2, and 3 monoclonal antibody on wound healing and hypertrophic scar formation. *J Am Coll Surg* 2005;201:391–397.
25. Coker RK, Laurent GJ, Shahzeidi S, Lympany PA, du Bois RM, Jeffery PK, *et al*. Transforming growth factors-β1, -β2, and -β3 stimulate fibroblast procollagen production in vitro but are differentially expressed during bleomycin-induced lung fibrosis. *Am J Pathol* 1997;150:981–991.
26. Andreola F, Calvisi DF, Elizondo G, Jakowlew SB, Mariano J, Gonzalez FJ, *et al*. Reversal of liver fibrosis in aryl hydrocarbon receptor null mice by dietary vitamin A depletion. *Hepatology* 2004;39:157–166.
27. Akhurst RJ, Hata A. Targeting the TGFβ signalling pathway in disease. *Nat Rev Drug Discov* 2012;11:790–811.
28. Badri KR, Yue M, Carretero OA, Aramgam SL, Cao J, Sharkady S, *et al*. Blood pressure homeostasis is maintained by a P311–TGF-β axis. *J Clin Invest* 2013;123:4502–4512.
29. Studler JM, Glowinski J, Lévi-Strauss M. An abundant mRNA of the embryonic brain persists at a high level in cerebellum, hippocampus and olfactory bulb during adulthood. *Eur J Neurosci* 1993;5:614–623.
30. Pan D, Zhe X, Jakkaraju S, Taylor GA, Schuger L. P311 induces a TGF-β1-independent, nonfibrogenic myofibroblast phenotype. *J Clin Invest* 2002;110:1349–1358.
31. Fujitani M, Yamagishi S, Che YH, Hata K, Kubo T, Ino H, *et al*. P311 accelerates nerve regeneration of the axotomized facial nerve. *J Neurochem* 2004;91:737–744.
32. Zhao L, Leung JK, Yamamoto H, Goswami S, Kheradmand F, Vu TH. Identification of P311 as a potential gene regulating alveolar generation. *Am J Respir Cell Mol Biol* 2006;35:48–54.
33. Tan J, Peng X, Luo G, Ma B, Cao C, He W, *et al*. Investigating the role of P311 in the hypertrophic scar. *PLoS One* 2010;5:e9995.
34. Hirano M, Sato K, Tanaka S, Tai Y, Inoue Y, Kiyokawa K, *et al*. [Surgery of the anterior skull base for head and neck tumors [in Japanese]. *Nippon Jibiinkoka Gakkai Kaiho* 1991;94:343–350.
35. Petrie RJ, Yamada KM. Fibroblasts lead the way: a unified view of 3D cell motility. *Trends Cell Biol* 2015;25:666–674.
36. Mariani L, McDonough WS, Hoelzinger DB, Beaudry C, Kaczmarek E, Coons SW, *et al*. Identification and validation of P311 as a glioblastoma invasion gene using laser capture microdissection. *Cancer Res* 2001;61: 4190–4196.
37. Shi J, Badri KR, Choudhury R, Schuger L. P311-induced myofibroblasts exhibit ameboid-like migration through RalA activation. *Exp Cell Res* 2006;312:3432–3442.
38. Taylor GA, Rodriguiz RM, Greene RI, Daniell X, Henry SC, Crooks KR, *et al*. Behavioral characterization of P311 knockout mice. *Genes Brain Behav* 2008;7:786–795.
39. Sun YG, Gao YJ, Zhao ZQ, Huang B, Yin J, Taylor GA, *et al*. Involvement of P311 in the affective, but not in the sensory component of pain. *Mol Pain* 2008;4:23.
40. Yue MM, Lv K, Meredith SC, Martindale JL, Gorospe M, Schuger L. Novel RNA-binding protein P311 binds eukaryotic translation initiation factor 3 subunit b (eIF3b) to promote translation of transforming growth factor β1-3 (TGF-β1-3). *J Biol Chem* 2014;289: 33971–33983.
41. Akhurst RJ. Targeting TGF-β signaling for therapeutic gain. *Cold Spring Harb Perspect Biol* 2017;9:a022301.
42. Gao L, Yue MM, Davis J, Hyjek E, Schuger L. In pulmonary lymphangioleiomyomatosis expression of progesterone receptor is frequently higher than that of estrogen receptor. *Virchows Arch* 2014; 464:495–503.
43. Zhang H, Neuhöfer P, Song L, Rabe B, Lesina M, Kurkowski MU, *et al*. IL-6 trans-signaling promotes pancreatitis-associated lung injury and lethality. *J Clin Invest* 2013;123:1019–1031.
44. Richeldi L, du Bois RM, Raghu G, Azuma A, Brown KK, Costabel U, *et al*.; INPULSIS Trial Investigators. Efficacy and safety of nintedanib in idiopathic pulmonary fibrosis. *N Engl J Med* 2014;370:2071–2082.
45. King TE Jr, Bradford WZ, Castro-Bernardini S, Fagan EA, Glaspole I, Glassberg MK, *et al*.; ASCEND Study Group. A phase 3 trial of pirfenidone in patients with idiopathic pulmonary fibrosis. *N Engl J Med* 2014;370:2083–2092.
46. Richeldi L, Kreuter M, Selman M, Crestani B, Kirsten AM, Wuyts WA, *et al*. Long-term treatment of patients with idiopathic pulmonary fibrosis with nintedanib: results from the TOMORROW trial and its open-label extension. *Thorax* 2018;73:581–583.
47. Zhou L, Dong X, Wang L, Shan L, Li T, Xu W, *et al*. Casticin attenuates liver fibrosis and hepatic stellate cell activation by blocking TGF-β/Smad signaling pathway. *Oncotarget* 2017;8:56267–56280.
48. Su SA, Yang D, Wu Y, Xie Y, Zhu W, Cai Z, *et al*. EphrinB2 regulates cardiac fibrosis through modulating the interaction of Stat3 and TGF-β/Smad3 signaling. *Circ Res* 2017;121:617–627.
49. Tu X, Zhang Y, Zheng X, Deng J, Li H, Kang Z, *et al*. TGF-β-induced hepatocyte lincRNA-p21 contributes to liver fibrosis in mice. *Sci Rep* 2017;7:2957.

50. Khalil H, Kanisicak O, Prasad V, Correll RN, Fu X, Schips T, *et al*. Fibroblast-specific TGF-β-Smad2/3 signaling underlies cardiac fibrosis. *J Clin Invest* 2017;127:3770–3783.
51. Oda K, Yatera K, Izumi H, Ishimoto H, Yamada S, Nakao H, *et al*. Profibrotic role of WNT10A via TGF-β signaling in idiopathic pulmonary fibrosis. *Respir Res* 2016;17:39.
52. Guan S, Zhou J. Frizzled-7 mediates TGF-β-induced pulmonary fibrosis by transmitting non-canonical Wnt signaling. *Exp Cell Res* 2017;359:226–234.
53. Wei Y, Kim TJ, Peng DH, Duan D, Gibbons DL, Yamauchi M, *et al*. Fibroblast-specific inhibition of TGF-β1 signaling attenuates lung and tumor fibrosis. *J Clin Invest* 2017;127:3675–3688.
54. Srour N, Thébaud B. Mesenchymal stromal cells in animal bleomycin pulmonary fibrosis models: a systematic review. *Stem Cells Transl Med* 2015;4:1500–1510.
55. Wollin L, Wex E, Pautsch A, Schnapp G, Hostettler KE, Stowasser S, *et al*. Mode of action of nintedanib in the treatment of idiopathic pulmonary fibrosis. *Eur Respir J* 2015;45:1434–1445.
56. Trivedi R, Redente EF, Thakur A, Riches DW, Kompella UB. Local delivery of biodegradable pirfenidone nanoparticles ameliorates bleomycin-induced pulmonary fibrosis in mice. *Nanotechnology* 2012;23:505101.
57. Yao Z, Yang S, He W, Li L, Xu R, Zhang X, *et al*. P311 promotes renal fibrosis via TGFβ1/Smad signaling. *Sci Rep* 2015;5:17032.
58. Petrie RJ, Yamada KM. At the leading edge of three-dimensional cell migration. *J Cell Sci* 2012;125:5917–5926.
59. Massagué J, Chen YG. Controlling TGF-β signaling. *Genes Dev* 2000; 14:627–644.
60. Annes JP, Munger JS, Rifkin DB. Making sense of latent TGFβ activation. *J Cell Sci* 2003;116:217–224.
61. Chang HY, Chi JT, Dudoit S, Bondre C, van de Rijn M, Botstein D, *et al*. Diversity, topographic differentiation, and positional memory in human fibroblasts. *Proc Natl Acad Sci USA* 2002;99:12877–12882.
62. Nolte SV, Xu W, Rennekampff HO, Rodemann HP. Diversity of fibroblasts – a review on implications for skin tissue engineering. *Cells Tissues Organs* 2008;187:165–176.
63. Soldatov NM. Molecular diversity of L-type Ca^{2+} channel transcripts in human fibroblasts. *Proc Natl Acad Sci USA* 1992; 89:4628–4632.
64. Li H, Duann P, Lin PH, Zhao L, Fan Z, Tan T, *et al*. Modulation of wound healing and scar formation by MG53 protein-mediated cell membrane repair. *J Biol Chem* 2015;290:24592–24603.
65. Zeisberg M, Kalluri R. Cellular mechanisms of tissue fibrosis. 1. Common and organ-specific mechanisms associated with tissue fibrosis. *Am J Physiol Cell Physiol* 2013;304:C216–C225.
66. Betensley A, Sharif R, Karamichos D. A systematic review of the role of dysfunctional wound healing in the pathogenesis and treatment of idiopathic pulmonary fibrosis. *J Clin Med* 2016;6:E2.